

STI ATI No. 194424
ASTIA FILE COPY

UNITED STATES ATOMIC ENERGY COMMISSION

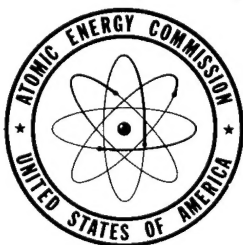
AECD-3456

CONSTITUTION DIAGRAM OF THE COPPER-
ZIRCONIUM ALLOY SYSTEM

By
Richard Norman Augustson

December 20, 1950

Ames Laboratory, Iowa State Coll.



DISSEMINATION STATEMENT A

Approved for public release
Distribution Unlimited

Technical Information Service, Oak Ridge, Tennessee

DTIC QUALITY INSPECTED 3

19970124 047

METALLURGY AND CERAMICS

~~PRINTED IN USA~~
~~PRICE 35 CENTS~~
Available from the
Office of Technical Services
Department of Commerce
Washington 25, D. C.

Other issues of this report may
bear the number ISC-138.

Work performed under
Contract No. W-7405-eng-82.

Date Declassified: October 20, 1952.

CONSTITUTION DIAGRAM OF THE COPPER-ZIRCONIUM ALLOY SYSTEM*

by

Richard Norman Augustson

I. ABSTRACT

The major aims of this investigation were to determine the constitution diagram of the copper-zirconium alloy system in the zirconium-rich region and to evaluate the hardness properties of the alloys prepared.

The following conclusions summarize the accomplishment of these aims.

1. In the copper-zirconium alloy system, with zirconium content above 60 weight-percent, an intermetallic compound, identified as CuZr_2 and having a melting point of 1065°C , was located at 73.6 percent zirconium. The crystal structure of this compound is body-centered tetragonal, with unit cell dimensions of $c = 11.3 \pm 0.2 \text{ \AA}$ and $a = 3.3 \pm 0.2 \text{ \AA}$.
2. A eutectic between CuZr_2 and zirconium was located at 80.3 percent zirconium with a eutectic temperature of 998°C .
3. A eutectoid was located at 95.0 ± 0.5 percent zirconium and $916 \pm 15^\circ\text{C}$.
4. No pyrrhoric alloys were encountered in the region studied.
5. The addition of even very small amounts of copper to zirconium was found to give an alloy harder than that of the zirconium itself, and the hardness rose, in general, with increased copper concentration.
6. The extent to which oxygen has altered the various transformation temperatures herein reported, or increased the hardness. Only the possibilities can be acknowledged at this time.

II. INTRODUCTION

Whereas the influence of limited amounts of zirconium on the properties of metals has been a subject of wide interest in metallurgy and its fields of application for many years, the influence of metals on the zirconium itself only recently has become of interest and importance.

One of the best methods available for producing pure zirconium metal at the present time, though at a relatively high cost, is the crystal-bar or iodide process. Tests have shown that this zirconium has desirable nuclear properties and good ductility but that it has insufficient strength at elevated temperatures for certain specific applications.

In view of these factors and of the high cost of the pure metal, alloys of zirconium offer the best possibilities of improving the above properties, especially the high-temperature strength, and thereby giving a more serviceable metal for nuclear reactors.

The purposes of the work herein described were to determine the constitution diagram of the binary alloy system of copper and zirconium in the zirconium-rich range, beyond that completed by earlier workers, and to determine the hardness of this range of alloys.

* M.S. thesis submitted December 1950. This work was performed under the direction of Dr. Harley A. Wilhelm.

The methods of procedure and equipment used in this investigation, the results and their interpretation, and the conclusions reached are discussed in the appropriate subsequent sections.

III. REVIEW OF THE LITERATURE

A survey of the literature for reports of investigation of the copper-zirconium alloy system revealed that the completion of the constitution diagram beyond 68 percent zirconium never was accomplished and that the zirconium-rich end of this system remained essentially untouched, probably because of a lack of material and suitable equipment.

As early as 1914 Hodgkinson (12) alloyed copper with several metals, including zirconium, by reducing the halide of zirconium with calcium carbide. In 1927 Boer (4) reported that alloys of zirconium with other metals besides aluminum could be formed by heating the metals together, but he warned of the danger of alloy contamination with carbon, silicon, phosphorus, and boron, all of which readily form zirconium compounds.

Allibone and Sykes (1, 9) were the first to study the system to any extent. In 1928 they reported the preparation of copper-zirconium alloys up to 35 percent zirconium by inductively heating the metals in an alundum crucible *in vacuo*. They found that near 30 percent copper the alloys acquired a sandy nature and could not be polished. A eutectic concentration was found at about 12.5 percent zirconium, melting at 964°C. An alloy of 30.55 percent zirconium still showed a small amount of eutectic with a primary compound phase, identified as Cu_3Zr , melting above 1000°C. Further work by Sykes (18) the following year indicated that the commercial application of these alloys appeared limited.

In 1937 Comstock and Bannon (6) made a series of copper-zirconium alloys, containing no more than 4 percent zirconium, for an investigation of temper-hardening and found that the maximum hardness of the alloy was obtained by tempering for 24 hours at 850°F an alloy which previously had been quenched.

Hensel, Larson, and Doty (11) reinvestigated in 1939 part of the system on the copper-rich side and found a eutectic composition at 12.5 percent zirconium with a eutectic temperature of 966°C. This agreed well with the earlier findings of Allibone and Sykes. Also, they found improvement in conductivity and increase in hardness by quenching and aging. They reported the limit of solid solubility to be about 0.3 percent zirconium.

Pogodin and co-workers (14,15) in 1940 published a phase diagram for the copper-zirconium system up to 36 percent zirconium as a result of thermal analyses and microstructure studies. They reported the presence of the compound Cu_3Zr at 32.65 percent zirconium with a melting point of 1140°C, and they confirmed earlier findings (1,9,11) of a eutectic of this compound with copper containing 12.9 percent zirconium with a melting point of 980°C. They found also that alloys near the compound were very brittle and that the hardness increased, while the electrical conductivity decreased, with increasing zirconium content.

To date the most extensive work on the copper-zirconium system is that of Raub and Engel (17). In 1948 they published the diagram and various thermal and mechanical data for alloys up to 68.3 percent zirconium. They reported two eutectics, one at 13.7 percent zirconium and 977°C, and the other at 51 percent zirconium and 877°C, and they placed the compound Cu_3Zr at 32.2 percent zirconium with a melting point of 1010°C. This last temperature is considerable lower than that given by Pogodin (14,15).

In a 1949 Atomic Energy Commission publication by Boulger (5), in an extensive review of zirconium metal, included tentative notes on the microstructures of a few as-cast copper-zirconium alloys prepared in graphite. He reported the presence of a eutectoid structure up to 15 percent copper, the highest alloy cast.

A preliminary survey of zirconium alloys published early in 1950 by the United States Bureau of Mines (2) included limited information on the microstructures and physical properties of several copper-zirconium alloys in the high zirconium range. The microstructure of the alloys showed that they were two-phase over the range studied and that a eutectic or eutectoid structure appeared present near 2 percent copper.

Throughout the years since 1928 a number of patents, such as issued to Belozerskii (3), Field (7), Guertler (8), Hensel (10), Philips (13), and Von Zeppelin (19), claimed various methods for preparing copper-zirconium alloys for commercial applications. However, these alloys contained only small amounts of zirconium metal.

IV. MATERIAL AND EQUIPMENT

As discussed in the subsequent section, Methods of Procedure, two methods were used for preparing the copper-zirconium alloys. The materials required for each of these methods are as follows:

Melting Method (in graphite crucible)

1. Copper metal, electrical grade, pieces cut from 2-inch rod.
2. Zirconium metal, sponge, prepared by the United States Bureau of Mines.
3. Argon gas, Matheson Chemical Company.

Bomb-Reduction Method

1. Copper metal, fine powder, reagent grade.
2. Zirconium tetrafluoride, resublimed, milled, prepared by the Ames Laboratory, Atomic Energy Commission.
3. Calcium metal, redistilled by the Ames Laboratory, Atomic Energy Commission.
4. Iodine, resublimed crystals, U.S.P.

The essential components of the induction furnace used for the preparation of alloys by the melting method and for the thermal analyses are shown in Figure 1. The sealed quartz tube was surrounded by a water-cooled induction coil. The quartz tube contained a packing of powdered graphite (Norblack) and a beryllia inner-liner which held the graphite crucible containing the charge.

The machined-graphite crucible, 1.5 inches internal diameter and 3 inches high, held a charge varying in weight from 150 to 200 grams. A 3-inch chimney, attached to the cover of the crucible, allowed the fumes to escape and permitted observation of the charge and temperature measurements to be made with an optical pyrometer through the window of optically flat pyrex glass in the head. Additional insulation in the form of insulating firebrick was placed above the permanent packing as shown in Figure 1.

Attached by means of heavy-walled vacuum tubing to the water-cooled head on the quartz tube was a Cenco-Hypervac-25 high vacuum pump, having an ultimate pressure of 0.1 micron. Operating pressures used during the various runs are tabulated in Table 2.

As shown in Figure 1, the leads from the converter were attached beneath the supporting platform. The converter used, a 20-kilowatt Ajax-Northrup, Type N, was a frequency changer designed to convert 60-cycle line current to high-frequency current of approximately 20,000 cycles.

A Stokes McLeod gage, having a range of 0-700 microns was used to measure the operating pressure in the quartz tube. It was attached downstream from a trap inserted ahead of the pump.

For alloys prepared by the bomb-reduction method, a steel bomb, 2.5 inches internal diameter and 12.5 inches high, with a screwed cap and a thermocouple well welded to the side, was used. A 2-inch fused dolomitic oxide liner shielded the charge from iron contamination. A simple drum-shaped gas-fired furnace, with the temperature controlled at 700°C by a Wheelco Potentiostat, was used for raising the bomb to the reaction temperature.

For recording thermal analysis readings, a Leeds and Northrup Micromax Recorder, Model S, was used. All thermocouples were made of 22-gauge chromel and alumel wires. The thermocouple bead was protected by a short beryllia insulator tube. Temperature readings were taken during the preparation of the alloys with a Leeds and Northrup optical pyrometer, having a range of 760°C to 2850°C on three scales.

The apparatus used for heating samples prior to quenching consisted of a 1-inch quartz tube, 30 inches long, and a Hevi-Duty Electric Company multiple-unit furnace, controlled by a Brown "Elektronik" controller. A vacuum of less than 0.1 micron was maintained during the

heating by means of a Distillation Products diffusion pump in series with a Welch "Duo-Seal" vacuum pump.

Hardness tests on specimens were made on a Rockwell Hardness Tester, using a 100 kilogram load for "B" scale readings. Knoop hardness tests were made on a Tukon Tester, with a Knoop indenter, a 16-millimeter objective, and a 500-gram weight.

The Tukon tester is used for indentation hardness tests with optical measurement of the indentation. Its use in this investigation made possible the determination of the relative hardness of separate phases in a single specimen. The Rockwell hardness measurement is an average hardness over a larger area.

Photomicrographs were made using a Bausch and Lomb research metallograph equipped with a tungsten-arc illuminating source. Standard metallurgical grinding and polishing wheels were used to prepare specimens for etching and examination. Specimens were examined with a Bausch and Lomb table-type metallurgical microscope.

The X-ray examinations of selected alloys were made with a North American Philips Company X-ray diffraction apparatus, consisting of a full-wave rectified generator and suitable controls. For this work a copper target and a nickel filter were used. Thus only copper K-alpha radiations were admitted to the powder camera.

V. METHODS OF PROCEDURE

A. Preparation of Alloys

The melting method, so designated because it involved melting together the desired amounts of metals in a machined graphite crucible, was used for the preparation of the majority of the alloys studied and for the thermal analyses of all of the alloys.

Figure 1 shows the location of such a crucible in position for heating in the induction furnace. The metals used for this method were in the form of small pieces, rather than fine powder, in order to prevent, as much as possible, oxidation of the metals. Zirconium metal, especially, is very readily oxidized at elevated temperatures. It acts as a powerful deoxidizer in copper melts and also picks up nitrogen readily to form nitrides. Oxygen is known to increase the hardness and strength of zirconium but to lower its ductility.

It was necessary to conduct the induction heating of the charge in two stages, first under an inert atmosphere of argon and then under a high vacuum. The use of this two-stage melting cycle was found necessary because of the extensive splattering of the charge as volatile material was boiled out of the zirconium sponge. This began to occur shortly above the melting point of the copper. A noticeable increase in fumes was evident at about 1110°C. In order to facilitate the removal of these impurities less violently the charge first was melted at atmospheric pressure under a stream of argon, which was vented through one of the thermocouple tubes shown in Figure 1.

Following the melting under argon the converter was shut off, and when the charge had solidified, a vacuum was pulled on the system. The second heating cycle was used to remove any remaining impurities and to allow thorough mixing of the metals. During both cycles records were made of the temperature, pressure, and converter voltage. Typical values are shown in Table 2. Also, as shown in this table, the carbon pickup from the crucible was low. Oxygen contamination in both bomb-reduced and graphite-cast zirconium, however, was much greater.

At the conclusion of the heating cycles the charge was allowed to cool slowly under vacuum to room temperature before the procedures of examination and testing were begun. This slow cooling had the advantage of allowing equilibrium to be reached between the phases and made possible a dependable correlation of microstructure and hardness measurements, both of which are dependent upon the specific heat treatment given the alloy.

Preparation of alloys by means of the bomb-reduction method was found to be not only a more rapid method, but also one which yielded a more homogeneous alloy. However, the limited quantities of zirconium tetrafluoride available during much of this investigation pre-

vented the use of the bomb-reduction method except for alloys with at least 90 percent zirconium.

The fine copper powder and milled zirconium tetrafluoride, in proper proportions to yield a 200-gram alloy biscuit, were mixed intimately with sufficient calcium metal filings and iodine crystals and placed in the lined steel bomb described in Section IV. The quantity of calcium was sufficient to react exothermally both with the iodine booster, to increase the temperature of the reaction, and with the zirconium tetrafluoride, which was reduced to zirconium and alloyed with the copper.

When the bomb was sealed and placed in the 700°C furnace, the highly exothermic reaction occurred near a bomb temperature of 600°C. No means was available for measuring the actual maximum temperature reached within the bomb, although the initiation of the reaction was noted by a sharp temperature rise in the thermocouple well welded to the outside of the bomb. Following this temperature surge the bomb was removed from the furnace and cooled before being opened. The compact alloy biscuit was found beneath the slag, which was mainly a mixture of calcium fluoride and calcium iodide, with possibly some unreacted iodine, calcium, and zirconium tetrafluoride.

B. Alloy Examination and Testing

Following the preparation of an alloy by either of the methods which have been described, the alloy biscuit was cleaned in preparation for a series of examinations. The only treatment necessary for a graphite-crucible alloy was a coarse grinding or buffing to remove the graphite remaining on the surface. The bomb-reduction alloys were soaked in dilute hydrochloric acid to remove the residual slag. A sample of each alloy, removed by a cut-off wheel, was submitted to the analytical laboratory for quantitative analysis. Originally each sample was analyzed both for copper and zirconium. However, it soon appeared evident that the results for percent zirconium, which included hafnium, were not reproducible. Therefore, the position of the alloy in the constitution diagram was based entirely upon the percent copper, as obtained by electrodeposition. Several analyses made for other elements, such as iron and carbon, are shown in Table 2.

Another sample of each alloy was mounted in Bakelite and prepared for an examination of the microstructure by the standard metallurgical grinding and polishing operations. Final lapping was made on a lapping wheel with 600-mesh levigated alumina, following which the sample was washed thoroughly and etched.

The etching operation was necessary in order to remove surface metal which was distorted or disturbed by the grinding operation, so that the true structure could be observed. Various common etchants were used without success on the copper-zirconium alloys, and only those containing hydrofluoric acid were found satisfactory. The etchant found most useful in this work contained 10 parts of hydrofluoric acid, 89 parts of water, and 1 part of concentrated nitric acid. The etching time increased from one or two seconds with the high-copper alloys to five or six seconds as the copper concentration decreased. Etching at best is a trial and error process with each sample requiring a slightly different treatment.

When a satisfactory etch was obtained, as determined by repeated microscopic examinations, a photomicrograph of the specimen was taken on the Bausch and Lomb metallograph. Section VI contains certain of the prints which were made.

Microstructure examinations, in addition to the one given the original as-cast or slow-cooled alloy, were made on selected alloy samples which had been annealed under vacuum for at least 20 hours and then quenched in water. The results and their interpretations are contained in subsequent sections.

The third important test to which a sample of each alloy was submitted was that of the thermal analysis. The equipment for this procedure has been described in Section IV. A sample of approximately 50 grams was cut into small pieces and packed around the shielded thermocouple in a graphite crucible. The crucible then was fitted into the quartz tube in the induction furnace and the alloy melted around the thermocouple junction. Chromel-alumel thermocouples were employed for temperature up to 1300°C. Alloys which had been observed

with the optical pyrometer to melt above this temperature were prepared for the thermal analysis simply by drilling a hole in a large piece and inserting the shielded thermocouple. Thus, weak thermal arrests in the cooling curve, especially near the eutectoid temperature, were more likely to be noted.

The thermocouple wires were protected by insulators and passed through the taps in the vacuum head of the induction furnace to lead wires from the recording instrument. A vacuum was then pulled on the sealed system before the induction furnace was turned on. As the sample was heated, the temperature change was recorded on the recording instrument. It was allowed to reach 1230°C and was maintained at that temperature for at least 15 minutes in order that the tube packing could reach a high enough temperature to insure a cooling rate of less than 10 degrees per minute. At high cooling rates slight temperature changes were not recorded. Cooling rates, 10 minutes after the converter had been shut off, are shown for these alloys in Table 1, together with temperatures on the cooling curves at which a thermal arrest or slope change was noted. The significance of such points is pointed out in Section VI, Results and Discussion. At least two cooling curves were recorded for each alloy, the final curve extending to room temperature.

Using the section of each alloy which had been polished and etched the Rockwell and Knoop hardness values were measured. Where possible, the hardness of each phase was measured on the Tukon tester as a means of identifying the phases. Results are listed in Section VI.

The final examination given to representative samples of these alloys was an X-ray examination in which a powder diagram was prepared. The results are discussed in Section VI. The equipment used for these X-ray examinations has been described. The preparatory procedure and operating technique was standard for such equipment. Fine filings of each sample were annealed at 600°C for 6 hours in a sealed quartz capillary with a short piece of zirconium foil enclosed to act as an oxygen "getter." A fine glass fiber, lightly coated with grease, was used to suspend the filings in the camera in line with the collimated X-ray beam. An exposure of 1.5 to 2 hours was adequate for the size of camera used. After the film had been developed the arcs of each powder diagram were measured and the $\sin^2 \theta$ values were found. Final indexing of the powder diagram of Alloy No. 17 and identification of the compound was made by the X-ray Laboratory. Results are given in the following section.

VI. RESULTS AND DISCUSSION

A proposed constitution diagram of the copper-zirconium alloy system above 50 weight percent zirconium is shown in Figure 2 as it has been deduced from a combination of alloy microstructure studies, thermal analyses, and the other alloy tests which have been described.

Of particular importance in this, as in any constitution diagram, are the location of compounds, eutectics, and eutectoids. One of each was found beyond the eutectic reported Raub and Engel (17) at 51 weight percent zirconium and 877°C. The compound, identified as CuZr_2 by X-ray analysis, is located at 73.6 percent zirconium. The eutectic is located at 80.3 percent zirconium and has a eutectic temperature of 998°C. Beyond this eutectic the liquidus curve rises smoothly to the melting point of zirconium, $1865 \pm 65^\circ\text{C}$. A eutectoid is located at 95.0 ± 0.5 percent zirconium and $916 \pm 15^\circ\text{C}$.

As indicated on the diagram, the limit of solid solubility in the lower region is subject to variation, although from the photomicrographs this limit certainly is less than 1.5 percent copper. This is supported further by the X-ray studies, which show little or no deviation of the zirconium $\sin^2 \theta$ values of the 18 percent copper alloy from the values obtained from the unalloyed bomb-reduction zirconium.

Table 1 lists the plotted thermal arrest values obtained by thermal analyses. As would be expected, the intensity of such points on a cooling curve were found to vary from sharp prolonged arrests in some alloys to only slight changes in slope in others. The solidus arrests weakened markedly as the alloy composition change in either direction on the diagram from that of the eutectic.

In contrast to the sharp thermal arrests of the eutectic thermal analyses, those of the

eutectoid were generally weak and sluggish, even near the eutectoid concentration. Consequently, greater reliance for this transformation was placed on the microstructure of quenched specimens.

For the highest grade of oxygen-free zirconium, a transformation temperature is known to be close to 865°C, where the solid-phase transformation from the hexagonal close-packed structure, alpha zirconium, to the face-centered cubic structure, beta zirconium takes place. However, oxygen, which dissolves readily and extensively in heated zirconium to form a solid solution, is known to raise this transformation temperature considerably (5). Even the bomb-reduction charges, which were flushed with argon as completely as possible before firing, were subject to extensive oxygen contamination. A great deal yet remains to be learned concerning the effects of oxygen on any zirconium alloy system, and the extent to which oxygen alters the resulting constitution diagram.

Table 2 gives data obtained during the vacuum-melting cycle of each alloy preparation. The pressures listed are those measured just prior to both the initiation and cessation of induction heating. The rise in pressure in all cases indicates continuing expulsion of volatile impurities from the charge. In runs where the maximum temperature exceeded 1200°C the pressure rise was more serious.

Alloy analyses, which determined the position of the alloy on the diagram, also are given in Table 2. With the exception of Alloy No. 2, which had excessive carbon contamination, the carbon contamination in the other samples checked was less than 0.1 percent.

The photomicrographs made of this series of alloys, necessary for the development of the constitution diagram, comprise Figures 3 to 55.

Figure 3 shows a microsection of the unalloyed bomb-reduction zirconium. The composition of the fine-grained precipitate at the grain boundaries is not known, but its presence is not uncommon in zirconium and its alloys. A sample of the same zirconium, annealed and quenched at 900°C is shown in Figure 4. No significant difference is noted over that of the unannealed specimen.

A definite change, however, above 900°C is evident in the sample annealed and quenched at 1050°C. Figures 5, 6, and 7 are all photomicrographs of the same specimen and show the variation which can be obtained. The fact that this series of zirconium photomicrographs ostensibly shows only a single phase must be remembered in examining the succeeding two-phase alloys.

Figures 8 through 13 comprise a series of photomicrographs of a 0.76 percent copper alloy with various heat treatments. Only minor difference exists between these specimens and the corresponding zirconium specimens which had the same heat treatment. Thus, the assumption is made that these alloys are in a region of solid solubility.

Figure 14, a slow cooled 1.51 percent copper alloy, prepared in graphite, shows the beginning of the eutectoid structure in place of the single-phase zirconium structure of the previous samples.

Figures 15 through 21 are a series of photomicrographs of a 1.72 percent copper alloy with various heat treatments. Somewhat more of the eutectoid structure occurs in the slow-cooled sample, Figure 15, than is present in Figure 14. Specimens quenched at 800°C, 854°C, and 900°C, Figures 16, 17, and 18, all are considered to contain eutectoid precipitation, modified or varying in each case with the annealing time and temperature. The sample shown in Figure 19, though containing the fine-grained precipitate peculiar to the single-phase alpha zirconium specimens as shown in Figure 9, is believed to exist in the region of alpha and beta zirconium shown in Figure 2. Likewise, the specimen of Figure 20, quenched at 950°C exists just inside this region and shows two clear phases.

A sample of the single-phase beta zirconium in the two-component region of solid solubility is shown in Figure 21 and was obtained by annealing and quenching a sample of the 1.72 percent copper alloy at 1075°C.

An unquenched sample of 2.04 percent copper alloy, prepared in graphite, is shown in Figure 22. Carbides probably make up the contaminating structure. The eutectoid structure of this sample, though somewhat coarser, is unchanged by annealing and quenching at 850°C. Although the 2.04 percent copper alloy of Figure 24 corresponds to the alloy of Figure 20, it is more heavily contaminated with carbides.

Figures 25 through 28 are photomicrographs after a series of heat treatments on a 3.25 percent copper alloy, prepared by bomb-reduction. The as-cast sample and those annealed at 800°C and 900°C show evidence of the peculiar, though not uncommon, metallurgical phenomenon known as coalescence, wherein the microstructure appears to be two well-separated phases and does not show a typical eutectoid structure. However, this generally occurs only at prolonged elevated temperatures, and absence of eutectoid in the as-cast sample is not explained. The 932°C sample of this series, Figure 28, appears decidedly altered from the samples treated at lower temperatures. The two clear phases would place it very close to the solid solution boundary in the alpha-beta zirconium region as shown in the constitution diagram, Figure 2.

Figure 29, a section of the 4.68 percent copper alloy, prepared by bomb reduction, shows the eutectoid structure occupying the majority of the field. Figure 30 shows this same sample after quenching at 854°C and again exhibits coalescence of the eutectoid. The sample of this series, quenched at 900°C appears very close to the one-phase region, yet it contains evidence of some fine-grained or coalesced eutectoid structure, whereas, the structure obtained by quenching at 1075°C is definitely of a single phase.

Interpretation of microstructures of specimens such as these which were subject to several altering influences, including the effects of impurities such as oxygen and obvious non-homogeneity in several cases upon the etched structures, can be misleading and without thermal or other supporting evidence becomes very difficult.

The series of photomicrographs, Figures 33 through 35 are considered to be at or very close to the eutectoid, with the eutectoid temperature between 850°C and 950°C. The presence of the irregular clear areas in this sample is indicative of incomplete homogeneity. This sample was prepared by graphite-crucible method, and the high melting temperature was reached for only a short period of time.

The structure of the 6.95 percent copper alloy with various heat treatments is shown in Figures 36 through 39. Again the phenomenon of coalescence is evident, especially in the 900°C annealed sample. According to the thermal analysis, this specimen should contain some eutectoid structure together with the CuZr_2 phase. The two clear phases of beta zirconium and CuZr_2 are evident in the sample treated at 932°C and show no eutectoid appearing in the primary phase. It is possible that part of the clear second phase is composed of hyper-eutectoid in addition to the CuZr_2 phase.

The appearance of a small amount of eutectic structure and a sharp thermal break at the eutectic temperature show that the alloy containing 8.62 percent copper, Figures 40 through 42, is just to the left of the solid solubility region, which as shown in Figure 2 extends from 0 to 7.5 percent copper at the eutectic temperature.

The alloy of Figures 43 and 44 contains 11.84 percent copper and shows that the amount of eutectic is increasing in quantity and density as the eutectic composition is approached. The sample of this alloy which was quenched above the eutectoid, but below the eutectic temperature, appears to have undergone some spheroidization.

The 12.7 percent copper alloy of Figures 45 and 46 indicate an increased quantity of the fine-grained eutectic structure in the slowly cooled sample and a coarser eutectic structure in the sample annealed at 854°C.

Figures 47 and 48 show the microstructure of the slowly cooled and quenched samples, respectively, of the 18.66 percent copper alloy. The amount of eutectic present indicates the proximity of the eutectic composition. Coarse-grained eutectic again appears in the sample quenched at 854°C.

Supported by very strong thermal arrests, the microstructure of Figures 49 and 50 show that this alloy essentially has the eutectic composition which has been set at 19.7 ± 0.5 percent copper or 80.3 ± 0.5 percent zirconium.

The compound CuZr_2 becomes the primary phase in the microstructure of the alloy of Figures 51 and 52. Again a coarser eutectic structure is obtained by annealing and quenching at 854°C.

The amount of compound phase increases in the alloy of Figure 53 having 24.58 percent copper. The eutectic is fine-grained and dispersed.

Figure 54 shows the well-defined structure of the 26.40 percent copper alloy, which is believed to be within 0.5 percent of the pure compound. The structure of contamination at the grain boundaries is not identified. X-ray analysis of the compound was made, and it was identified as CuZr_2 .

The final photomicrograph, Figure 55, shows the structure of the 48.23 percent copper alloy. This is very close to the 49 percent copper eutectic reported by Raub and Engel (17). The thermal analysis agrees with their findings.

Table 3 lists the hardness of the copper-zirconium alloys and the Bureau of Mines zirconium in terms of both Rockwell B and Knoop hardness values. All readings are the averages of a number of impressions made across each sample.

The Rockwell instrument measures the average hardness over a much greater area than the Knoop indenter and thus does not differentiate between phases in a specimen. The Rockwell B readings indicate that copper additions have a hardening effect upon the zirconium. As the concentration of the copper increases, the hardness values are seen to rise to a maximum near the eutectic concentration and then to decline.

The tabulated values of the Knoop hardness tests do not show any strong trend either in the primary or the eutectic (eutectoid) structure, though again the copper is seen to increase the hardness of zirconium.

The differentiation between phases in a specimen was not always sharp, and undoubtedly there was considerable overlapping, especially near the eutectic and eutectoid concentrations.

The primary phase hardness readings, after an initial sharp rise, decline gradually as the copper content approaches the eutectic concentration and then increase again as the primary phase becomes the compound instead of zirconium. The eutectic or eutectoid structure readings are lower than the associated primary phase readings and, except for low readings at the eutectic composition, are more uniform throughout this range than the primary phase readings. Alloy No. 18 has the composition of a eutectic reported by previous workers. This alloy was too brittle to permit any Rockwell B measurement.

The erratic hardness values obtained for some alloys within this range must be attributed to non-homogeneity of the specimens or to differences in the heat treatment which the alloy received during the preparation. Also, any contamination of an alloy with the oxide, carbide, or nitride of zirconium would affect the hardness readings. The strong affinity of zirconium for carbon, and especially for oxygen and nitrogen, is well known. The presence of carbides is evident in many of the photomicrographs. Such impurities were very difficult to eliminate entirely.

In view of the difficulty of differentiating between phases in many samples, the possibility of errors due to contamination, and the variation in heat treatment of the samples, all of which may have contributed to the variation in the readings obtained, it is not possible to attach strong significance to these results or to draw conclusions beyond those observations which have been made.

Table 4 lists the $\sin^2 \theta$ values of reflections obtained on x-ray powder diagrams of three copper-zirconium alloys across the range studied and the $\sin^2 \theta$ values of Bureau of Mines zirconium. Values have been paired as closely as possible, so that segregation of the lines into those contributed by zirconium or by the compound can be made. The single values can be attributed to impurities or to conditions which caused a reflection to be present in one sample and absent in another.

On the basis of these tabulated values several observations can be made.

1. Zirconium metal is indicated as being the primary phase in Alloy No. 2, which contained 1.51 percent copper. The possibility of extensive solubility of the copper in the zirconium is reduced by the reasonable agreement of these values with those of pure zirconium.

2. Weaker but positive zirconium lines exist in the eutectic alloy, Alloy No. 14, having 19.72 percent copper. This reduced the possibility of any compound existing between this eutectic and the pure zirconium.

3. Only a few of the strongest zirconium lines appear in the powder diagram of Alloy No. 17, since this alloy is the compound, CuZr_2 . Likewise, lines contributed by the compound are strong in the eutectic powder diagram but very weak in the powder diagram of Alloy No. 2

which is very close to the pure zirconium.

Final X-ray examination of Alloy No. 17 was made in the Atomic Energy Commission X-ray Laboratory by Mr. Paul H. Lewis in order to confirm the chemical composition and to determine the unit cell data.

The following results are reported:

Chemical Composition:	CuZr_2
Specific Gravity:	6.98
Crystal Structure:	Body-centered tetragonal
Cell Dimensions:	$c = 11.3 \pm 0.2 \text{ \AA}$ $a = 3.3 \pm 0.2 \text{ \AA}$
Molecules per unit cell:	2
Space Group:	$D_{4h}^{17} - 14/\text{mmm}$
Atom Positions:	Cu $000, \frac{1}{2}\frac{1}{2}\frac{1}{2}$ Zr $00Z, \frac{1}{2}\frac{1}{2}\frac{1}{2} + Z$ $00\bar{Z}, \frac{1}{2}\frac{1}{2}\frac{1}{2} - Z$ Where $Z = 0.342 \pm 0.002$

VII. SUMMARY

As stated in the introduction, the major aims of this investigation were to determine the constitution diagram of the copper-zirconium alloy system in the zirconium-rich region and to evaluate the hardness properties of the alloys prepared.

The following conclusions summarize the accomplishment of these aims.

1. In the copper-zirconium alloy system, with zirconium content above 60 weight-percent, an intermetallic compound, identified as CuZr_2 and having a melting point of 1065°C , was located at 73.6 percent zirconium. The crystal structure of this compound is body-centered tetragonal, with unit cell dimensions of $c = 11.3 \pm 0.2 \text{ \AA}$ and $a = 3.3 \pm 0.2 \text{ \AA}$.
2. A eutectic between CuZr_2 and zirconium was located at 80.3 percent zirconium with a eutectic temperature of 998°C .
3. A eutectoid was located at 95.0 ± 0.5 percent zirconium and $916 \pm 15^\circ\text{C}$.
4. No pyrophoric alloys were encountered in the region studied.
5. The addition of even very small amounts of copper to zirconium was found to give an alloy harder than that of the zirconium itself, and the hardness rose, in general, with increased copper concentration.
6. The extent to which oxygen has altered the various transformation temperatures herein reported, or increased the hardness of the alloys, was not considered specifically in this investigation. Only the possibilities can be acknowledged at this time.

VIII. LITERATURE CITED

1. Allibone, T. E. and Sykes, C. The alloys of zirconium. Jour. Inst. of Metals. 39:173-9. 1928.
2. Anderson, C. T., Hayes, E. T., Roberson, A. H., and Kroll, W. J. A preliminary survey of zirconium alloys. U. S. Bureau of Mines Report of Investigation, No. 4658. 1950.
3. Belozerskii, N. A., et al. Alloying columbium, zirconium, etc., with iron, chromium, etc. Russian Patent 54,976. 1939. Abstracted in Chem. Abst. 35:2802. 1941.
4. Boer, J. H. Zirconium. Ind. Engr. Chem. 19:1259. 1927.
5. Boulger, Francis W. The properties of zirconium. U. S. Atomic Energy Commission Document 2726. 1949.

6. Comstock, G. F. and Bannon, R. E. Notes on the hardness and conductivity of heat-treated copper castings alloyed with zirconium and beryllium. *Metals and Alloys*. 8:106-9. 1937.
7. Field, Alexander L. Alloy containing zirconium and copper. U. S. Patent 1,684,696. Sept. 18, 1928. Abstracted in *Chem. Abst.* 22:4455. 1928.
8. Guertler, Wm. Zirconium alloys. French Patent 771,176. Oct. 2, 1934. Abstracted in *Chem. Abst.* 29:722. 1935.
9. Hansen, Max. *Der Aufbau der Zweistofflegierungen*. p. 672-3. Berlin, Verlag von Julius Springer. 1936.
10. Hensel, F. R. and Larsen, E. I. Welding electrode. U. S. Patent 2,097,816. Nov. 2, 1937. Abstracted in *Chem. Abst.* 32:108. 1938.
11. Hensel, F. R., Larsen, E. I., and Doty, A. S. Copper-zirconium-cadmium bronze. *Metals and Alloys*. 10:372-380. 1939.
12. Hodgkinson, W. R. An application of calcium carbide in the formation of alloys. *Jour. Soc. Chem. Ind.* 33:446. 1914.
13. Philips, N. V. Metal wire. French Patent 836,017. 1939. Abstracted in *Chem. Abst.* 33:4952. 1939.
14. Pogodin, S. A., Shumova, I. S., and Kugucheva, F. A. Constitution and properties of copper-zirconium alloys (in French). *Compt. rend. acad. Sci. (U. S. S. R.)*. 27:670-2. 1940. (Original not available for examination; abstracted in *Chem. Abst.* 35:1745. 1941.)
15. Pogodin, S. A. and Shumova, I. S. Alloys of copper with zirconium (in French). *Ann. secteur anal. phys.-chim., Inst. chim. gen. (U. S. S. E.)*. 13:225-232. 1940. (Original not available for examination; abstracted in *Chem. Abst.* 37:4350. 1943.)
16. Raub, Ernst and Engel, Max. Self-igniting alloys. *Metallforschung*. 2:115-19. 1947.
17. Raub, Ernst and Engel, Max. Alloys of zirconium with copper, silver, and gold. *Z. Metallkunde*. 39:172-7. 1948.
18. Sykes, C. The alloys of zirconium II. *Jour. Inst. of Metals*. 41:179-190. 1929.
19. Von Zeppelin, H. Manufacture of alloys. U. S. Patent 2,250,687. July 29, 1941. Abstracted in *Chem. Abst.* 35:6921. 1941.

IX. ACKNOWLEDGMENT

For recommendations and assistance generously contributed during the pursuance of this investigation, the author expresses his especial appreciation to Dr. Harley A. Wilhelm and to Mr. David Peterson of the Ames Laboratory of the Atomic Energy Commission.

Table I—Thermal Analyses of Copper-Zirconium Alloys

Alloy No.	Percent Copper	Cooling* Rate, °C/min	Cooling Curve Thermal Arrests, °C		
A†	0.0	14.3		931	864
2	1.51	6.6	1675‡	949	916
3	1.72			951	916
4	2.04	9.7		928	
5	3.25		1415‡		
7	5.20	9.5	1470‡		916
8	6.95		1205	987	911
9	8.62	7.7	1218‡	997	916
			1188		
10	11.84	9.2	1140‡	994	918
			1144		
12	18.03	10.0	1038	998	916
13	18.66	7.3	1018	994	923
15	22.54	6.7	1041	998	
16	24.58	7.8	1070	998	
17	26.40	7.8	1065	998	
18	48.23	8.7	896		

*Cooling rate after 10 minutes.

†Bureau of Mines sponge zirconium.

‡Values obtained with optical pyrometer.

Table 2—Preparation of Copper-Zirconium Alloys

Alloy No.	Charge Weight, g	Pressure Range Microns	Maximum Temp. °C	Final % Copper	Percent Impurities, Wt.
A*	166.3 Zr	25-450	1725	0.0	1.040 O ₂ 0.0186 Fe
B†		Bomb		0.0	0.52 O ₂
1		Reduction			
		Bomb		0.76	
		Reduction			
2	147 Zr 3 Cu	60-175	1700	1.51	1.078 C
3	360 ZrF ₄ 4 Cu	Bomb		1.72	
	338 I ₂ 259 Ca	Reduction			
4	171.5 Zr 3.5 Cu	60-320	1565	2.04	
5	336 ZrF ₄ 6 Cu	Bomb		3.25	
	338 I ₂ 258 Ca	Reduction			
6	349 ZrF ₄ 10 Cu	Bomb		4.68	
	338 I ₂ 258 Ca	Reduction			
7	148.8 Zr 9.5 Cu	8-700	1545	5.20	
8	340 ZrF ₄ 14 Cu	Bomb		6.95	
	338 I ₂ 249 Ca	Reduction			
9	157.5 Zr 17.5 Cu	Atm. of Ar	1375	8.62	
10	124 Zr 18 Cu	6-690	1255	11.84	0.0384 C
11	131.5 Zr 18.8 Cu	0.75-400	1100	12.70	
12	147 Zr 28 Cu	25-60	1350	18.03	
13	146 Zr 36.5 Cu	17-70	1250	18.66	
14	175 Zr 25 Cu	30-150	1100	19.72	
15	132.6 Zr 37.4 Cu	40-60	1150	22.54	
16	129.3 Zr 40.7 Cu	40-90	1325	24.58	
17	150 Zr 50 Cu	30-150	1100	26.40	0.044B C
18	102 Zr 98 Cu	25-35	1070	48.23	

*Bureau of Mines sponge zirconium (remelted).

†Bomb-reduction zirconium.

Table 3—Hardness Measurements on Copper-Zirconium Alloys

Alloy No.	Percent Copper	Rockwell B Hardness 100 kg load	Knoop Hardness 0.5 kg load	
			Primary Phase	Eutectic or Eutectoid
A	0.0	81.5	220 (Zr)	
2	1.51		336	271
3	1.72	88.8	387	319
			361*	335*
4	2.04	86.7		262
6	4.68	91.1	394*	
7	5.20	90.6	359	244
9	8.62	97.0	323	268
11	12.70	94.9		280
12	18.03	95.1	304	282
13	18.66	97.5		229
14	19.72	97.9		225
15	22.54	98.3	295	
16	24.58	95.3		252*
17	26.40	82.9	374	
18	48.23			585

*Sample quenched from 854°C.

Table 4—X-ray Examination of Copper-Zirconium Alloys

Alloy No. 17 26.4% Cu $\text{Sin}^2 \theta$	Alloy No. 14 19.72% Cu $\text{Sin}^2 \theta$	Alloy No. 2 1.51% Cu $\text{Sin}^2 \theta$	Bureau of Mines Zr $\text{Sin}^2 \theta$
0.0631	0.0626		
.0772	.0760	.0756	.0756
	.0890	.0895	.0908
.0941	.0949		
		.0982	.0982
.1022			
.1086	.1072		
		.1104	
.1169	.1149		
.1288	.1261		
	.1643	.1588	.1669
.1732	.1732		
.1938			.2025
	.2270	.2248	
.2318	.2306		.2298
			.2505
	.2761	.2772	.2793
.2890	.2862		
	.3147	.3050	.3049
		.3163	.3190
		.3245	.3277
.3315	.3307		
		.3536	
			.3605
	.3908	.3917	.3943
.4046	.4016		
		.4330	.4349
.4458	.4470		
.4617	.4608		
	.5055	.5064	.5059
.5248	.5222		
		.5328	.5316
		.5501	.5547
.5616	.5632		
.5762			.5868
			.6210
.5952		.6012	
.6353	.6336		
	.6529	.6530	.6621
.6752	.6727		
		.6882	.6839
.7084	.7100		
		.7296	.7331
.7482	.7459		
		.7726	.7720
	.8610	.8616	.8620

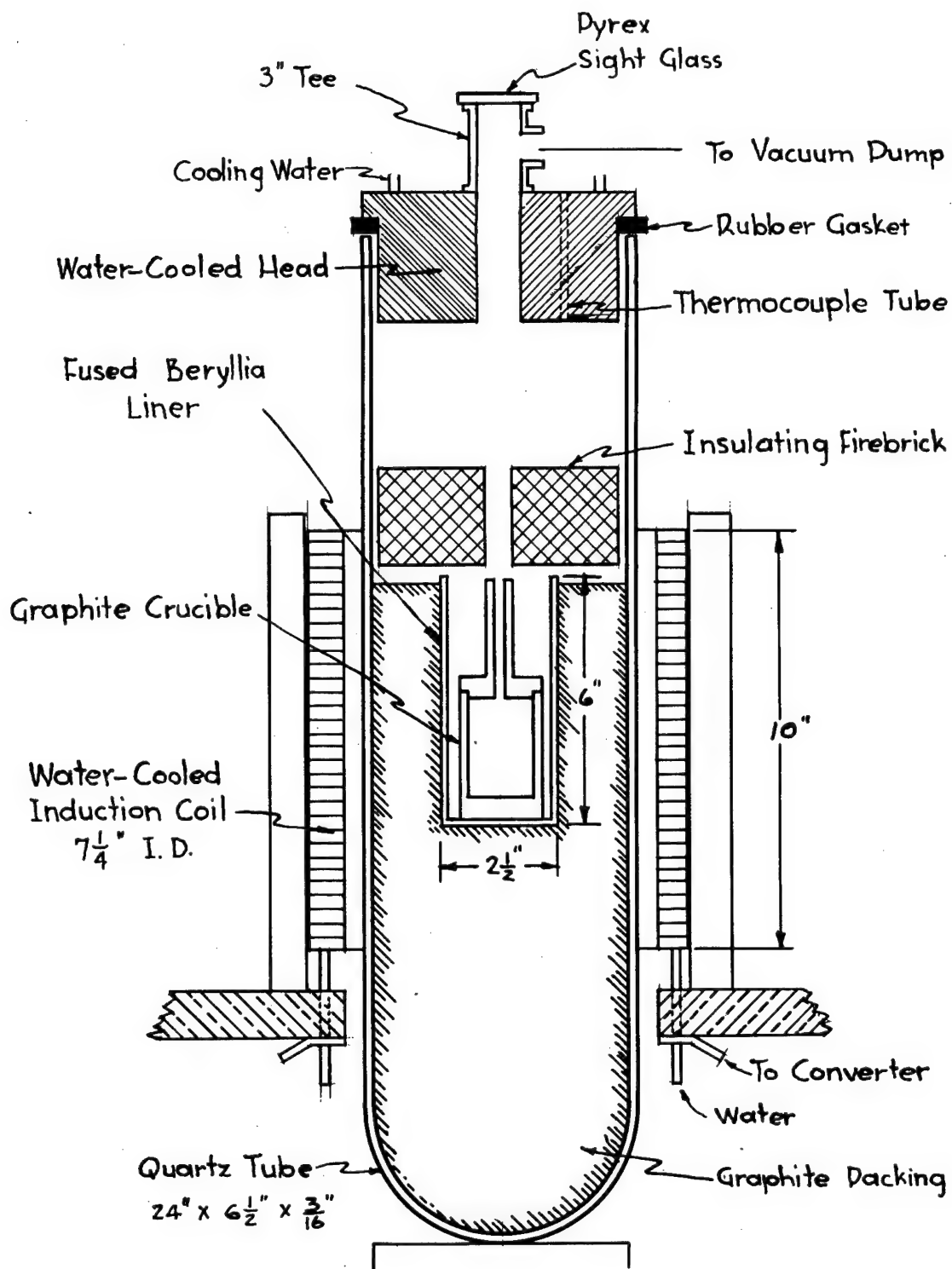


Fig. 1—Induction furnace.

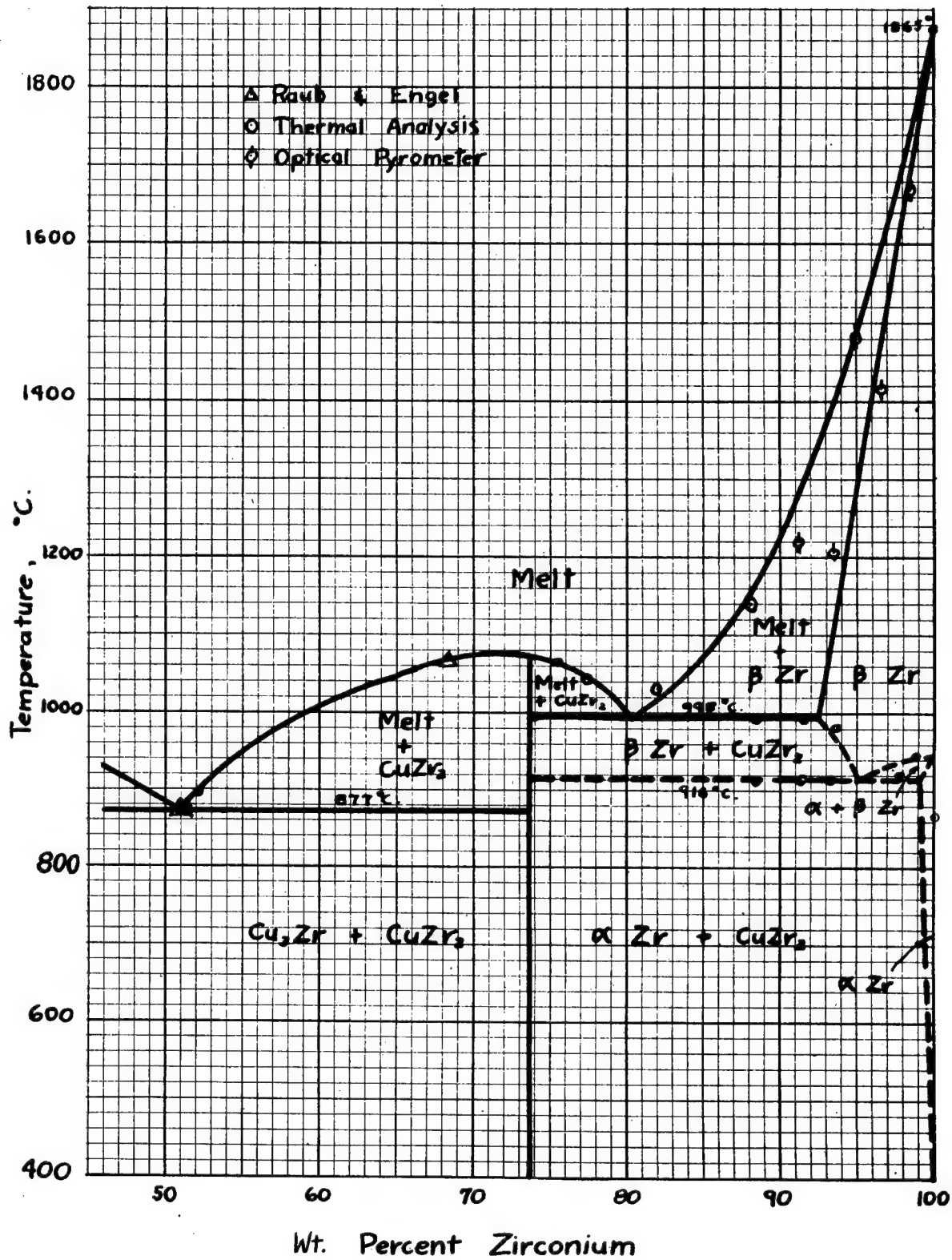


Fig. 2—Constitution diagram of the copper-zirconium alloy system.



Fig. 3—Zirconium metal (bomb-reduced).
150X.

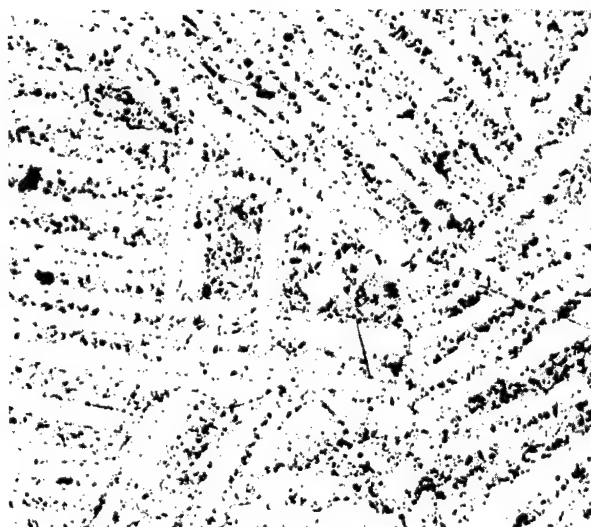
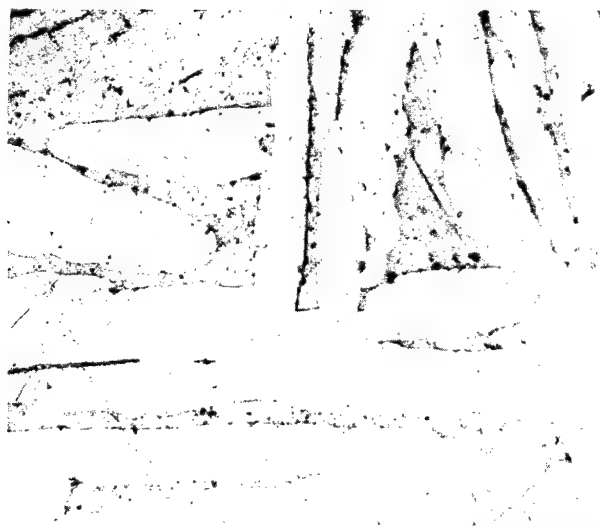
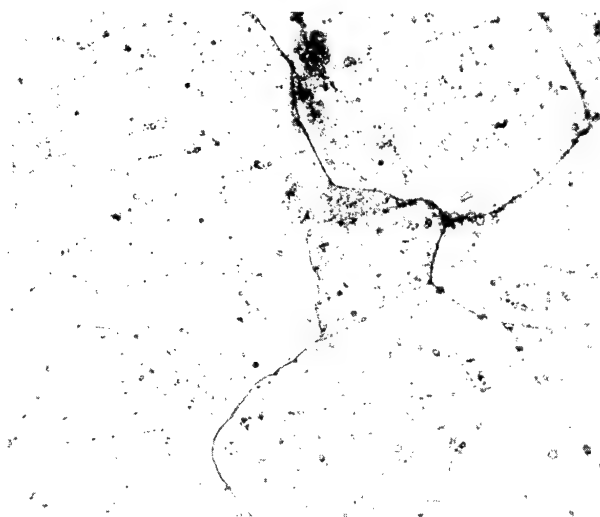


Fig. 4—Zirconium metal (bomb-reduced),
150X. Annealed and quenched at
900°C.



**Fig. 5—Zirconium metal (bomb-reduced).
150X. Annealed and quenched at
1075°C.**



**Fig. 6—Zirconium metal (bomb-reduced).
150X. Annealed and quenched at
1075°C.**

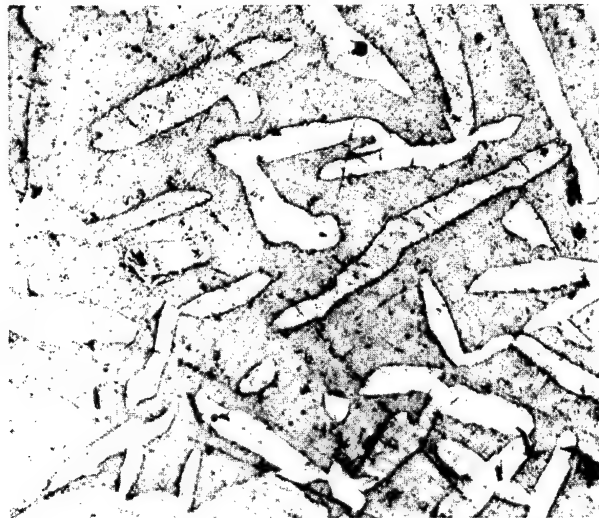


Fig. 7—Zirconium metal (bomb-reduced).
150X. Annealed and quenched at
1075°C.



Fig. 8—Copper-zirconium alloy (bomb-
reduced). 0.76% copper, 150X.

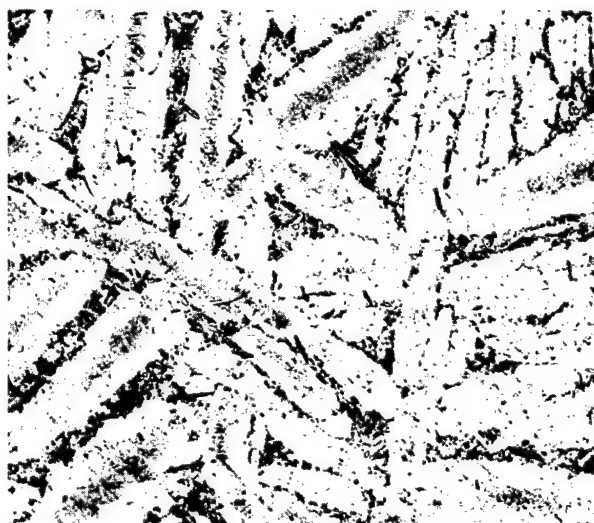


Fig. 9—Copper-zirconium alloy (bomb-reduced). 0.76% copper, 150X.
Annealed and quenched at 850°C.



Fig. 10—Copper-zirconium alloy (bomb-reduced). 0.76% copper, 150X.
Annealed and quenched at 900°C.

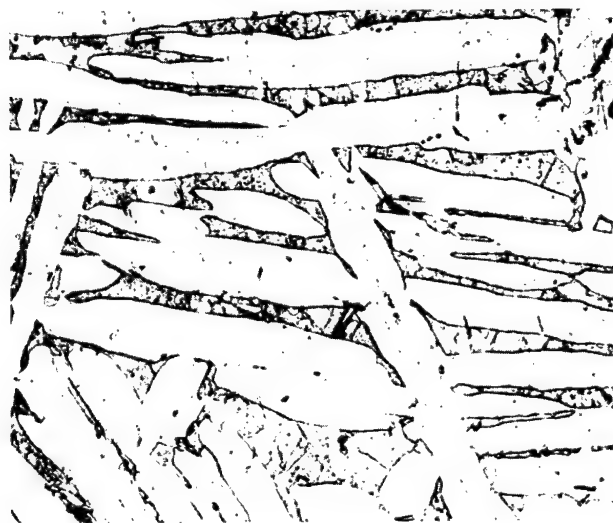


Fig. 11—Copper-zirconium alloy (bomb-reduced). 0.76% copper, 150X
Annealed and quenched at 920°C.

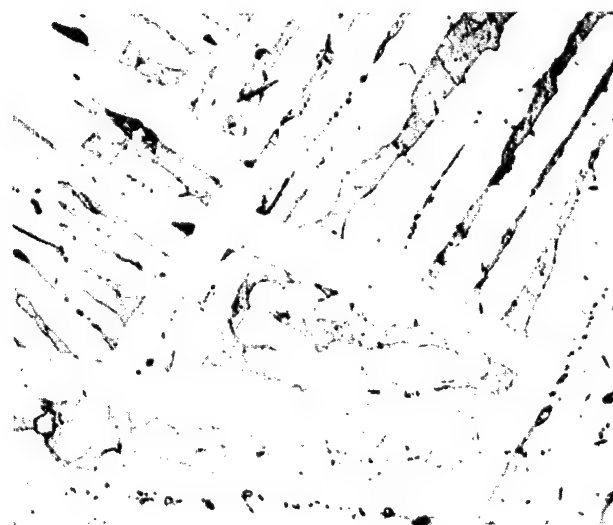


Fig. 12—Copper-zirconium alloy (bomb-reduced). 0.76% copper, 150X.
Annealed and quenched at 932°C.



**Fig. 13—Copper-zirconium alloy (bomb-reduced). 0.76% copper, 150X.
Annealed and quenched at 1075°C.**

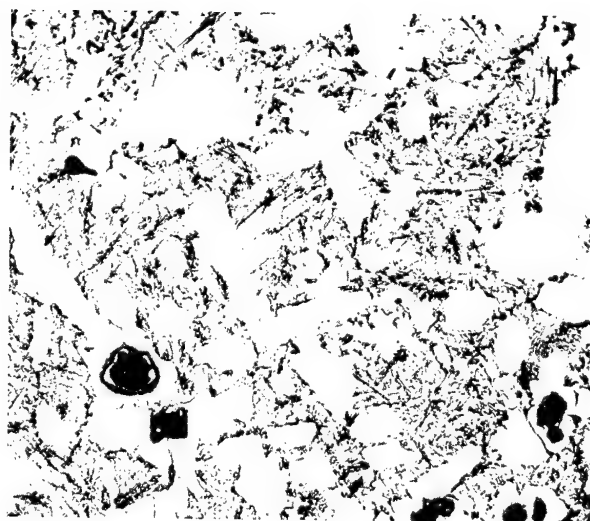


Fig. 14—Copper-zirconium alloy. 1.51% copper, 250X.



Fig. 15—Copper-zirconium alloy (bomb-reduced). 1.72% copper, 150X.

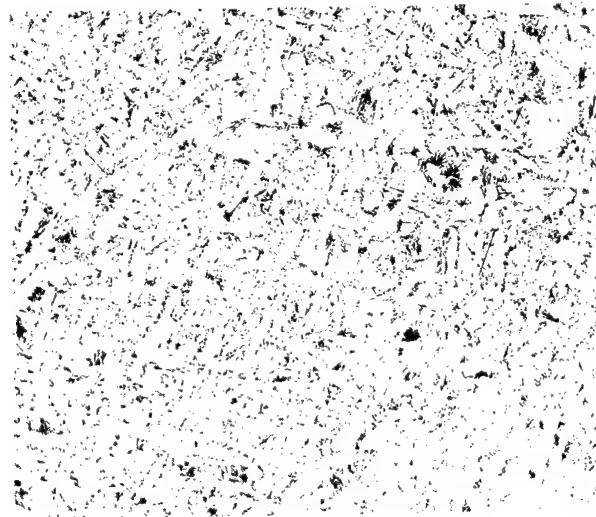


Fig. 16—Copper-zirconium alloy (bomb-reduced). 1.72% copper, 150X.
Annealed and quenched at 800°C.

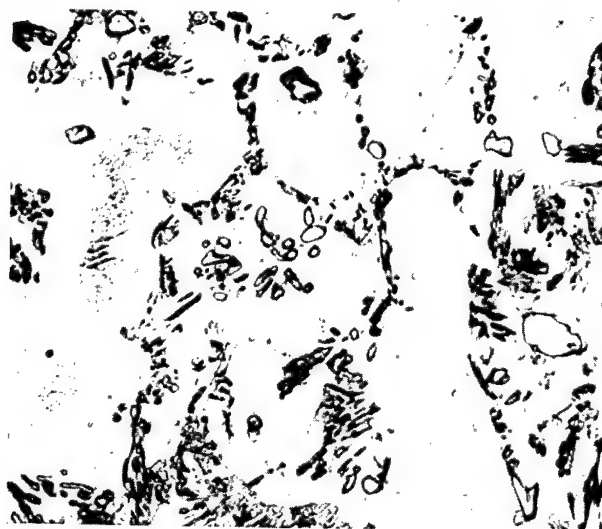


Fig. 17—Copper-zirconium alloy (bomb-reduced). 1.72% copper, 150X.
Annealed and quenched at 854°C.

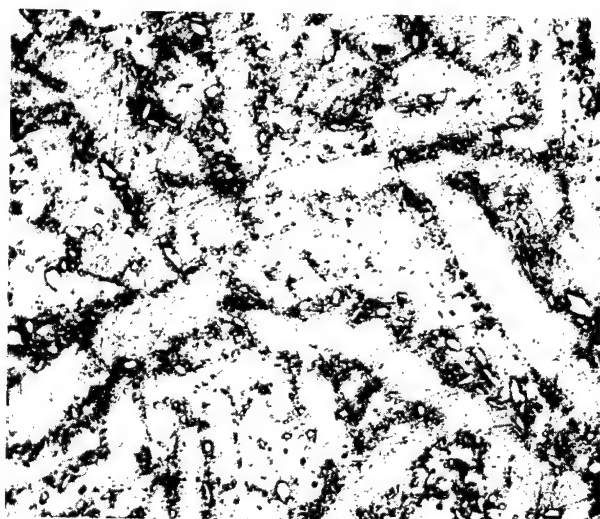


Fig. 18—Copper-zirconium alloy (bomb-reduced). 1.72% copper, 150X.
Annealed and quenched at 900°C.

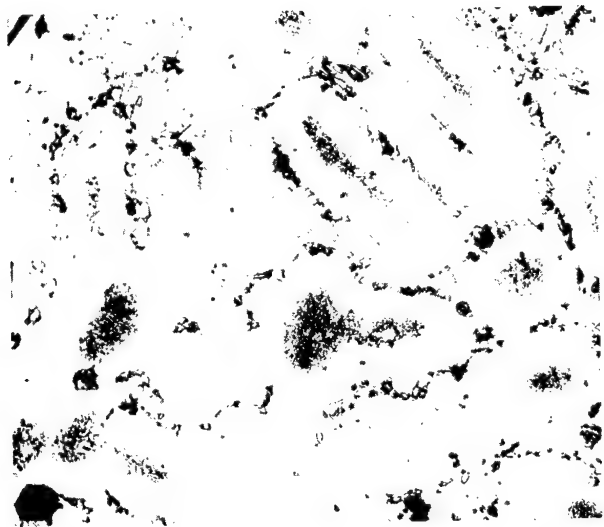


Fig. 19—Copper-zirconium alloy (bomb-reduced). 1.72% copper, 150X.
Annealed and quenched at 920°C.

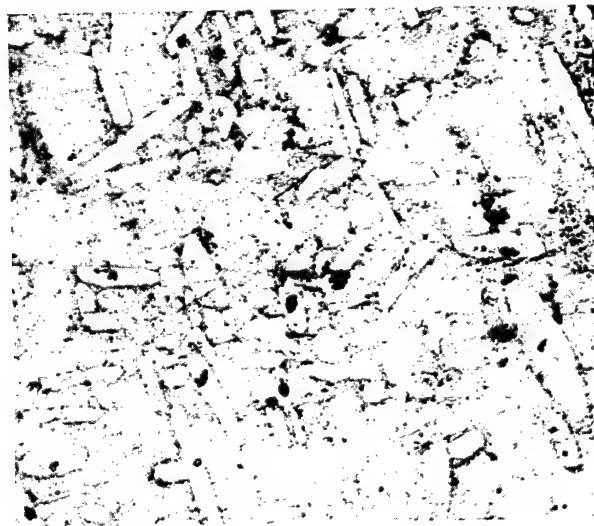


Fig. 20—Copper-zirconium alloy (bomb-reduced). 1.72% copper, 150X.
Annealed and quenched at 950°C.

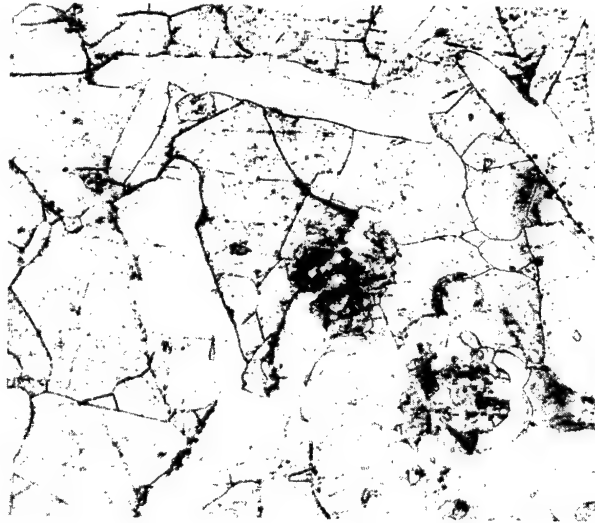


Fig. 21—Copper-zirconium alloy (bomb-reduced). 1.72% copper, 150X.
Annealed and quenched at 1075°C.

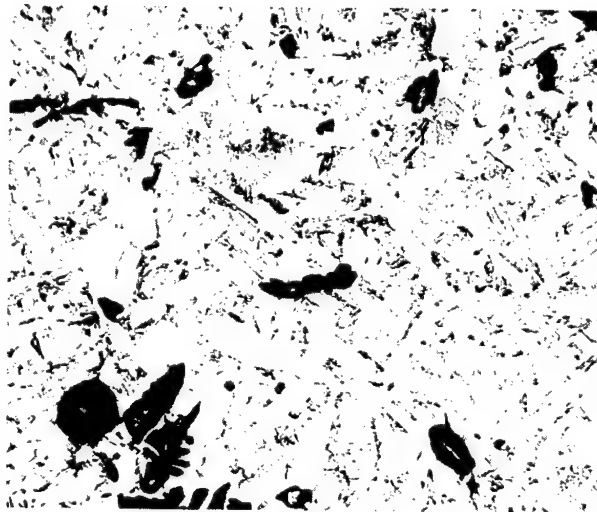


Fig. 22—Copper-zirconium alloy. 2.04% copper, 150X.

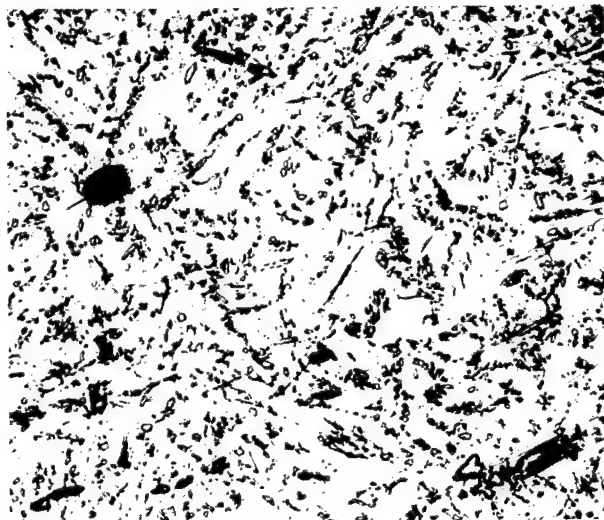


Fig. 23—Copper-zirconium alloy. 2.04% copper, 150X. Annealed and quenched at 850°C.

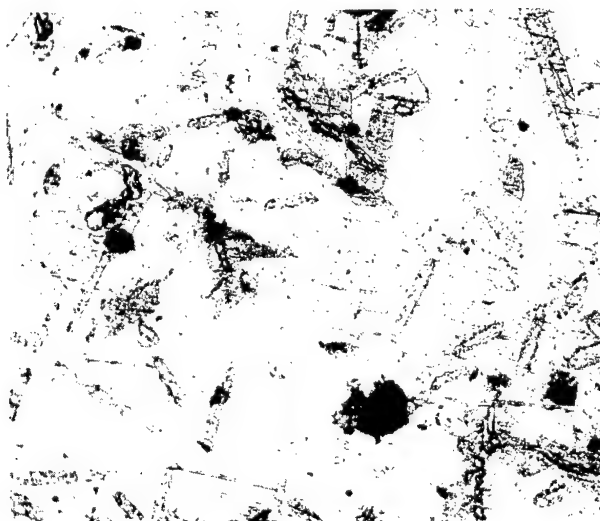


Fig. 24—Copper-zirconium alloy. 2.04% copper, 150X. Annealed and Annealed and quenched at 950°C.

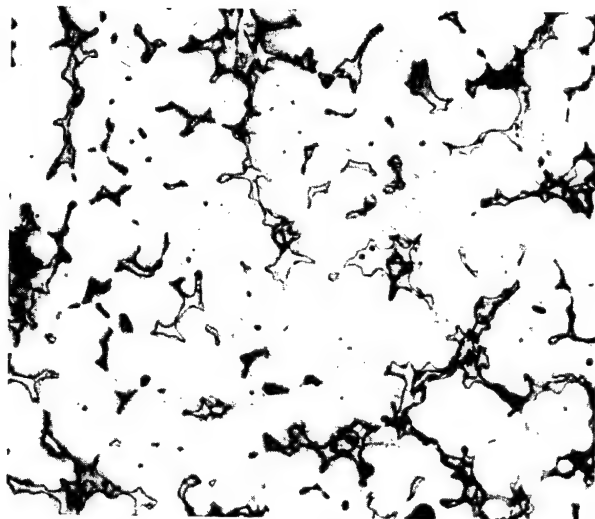


Fig. 25—Copper-zirconium alloy (bomb-reduced). 3.25% copper, 150X.

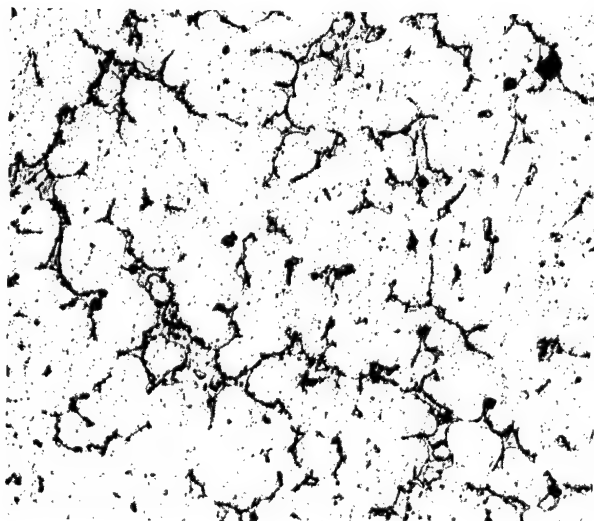


Fig. 26—Copper-zirconium alloy (bomb-reduced). 3.25% copper, 150X.
Annealed and quenched at 850°C.

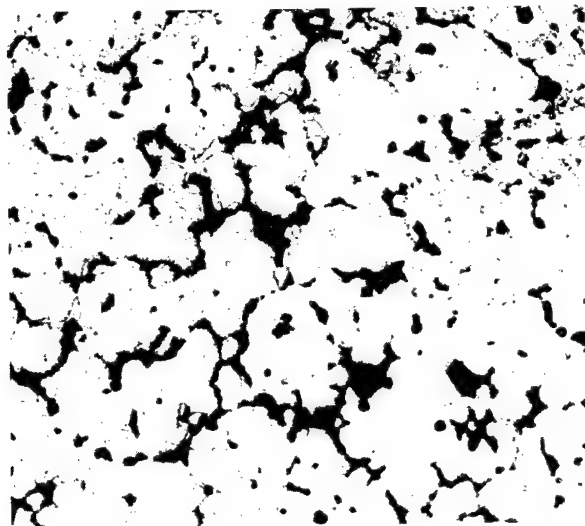


Fig. 27—Copper-zirconium alloy (bomb-reduced). 3.25% copper, 150X.
Annealed and quenched at 900°C.

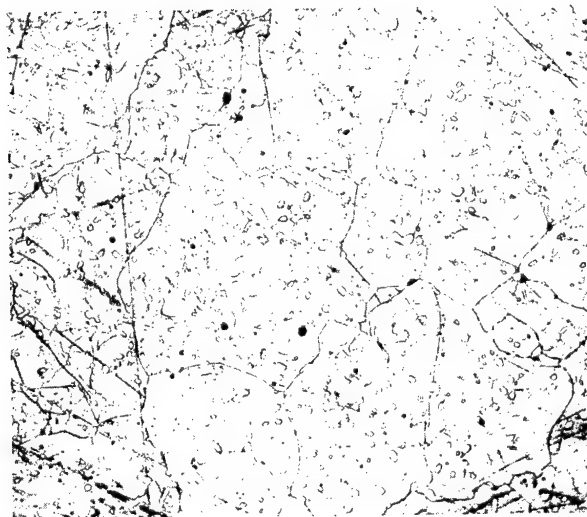


Fig. 28—Copper-zirconium alloy (bomb-reduced). 3.25% copper, 150X.
Annealed and quenched at 932°C.

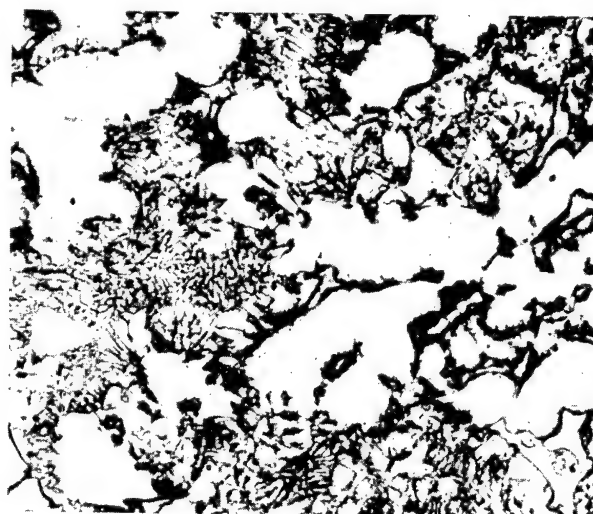


Fig. 29—Copper-zirconium alloy (bomb-reduced). 4.68% copper, 150X.

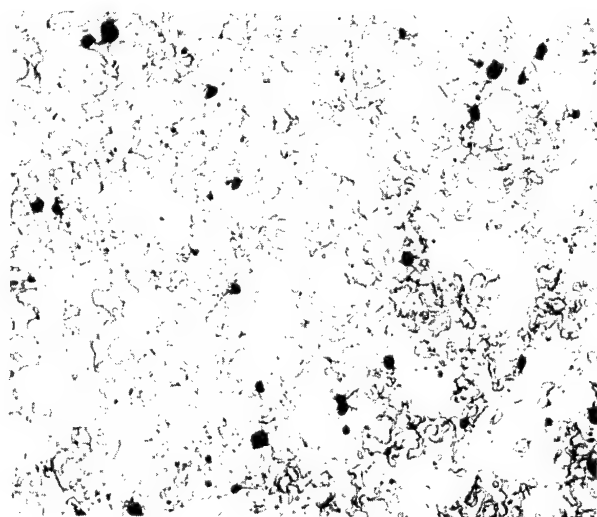


Fig. 30—Copper-zirconium alloy (bomb-reduced). 4.68% copper, 150X.
Annealed and quenched at 850°C.

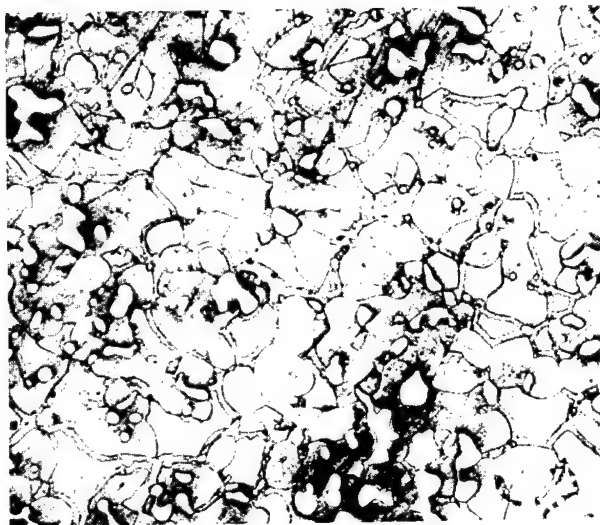


Fig. 31—Copper-zirconium alloy (bomb-reduced). 4.68% copper, 150X.
Annealed and quenched at 900°C.

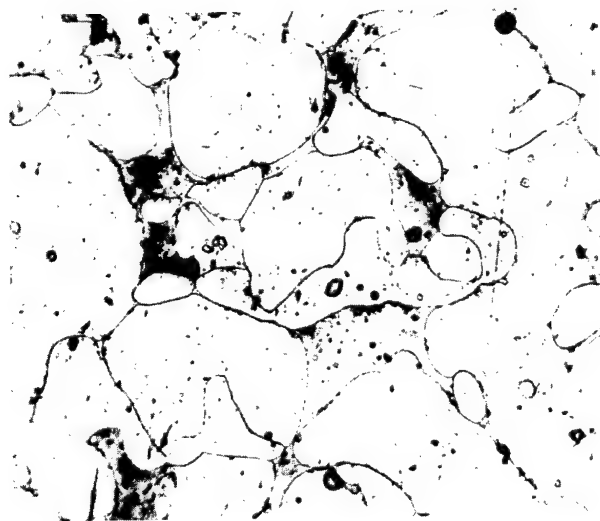


Fig. 32—Copper-zirconium alloy (bomb-reduced). 4.68% copper, 150X.
Annealed and quenched at 1075°C.

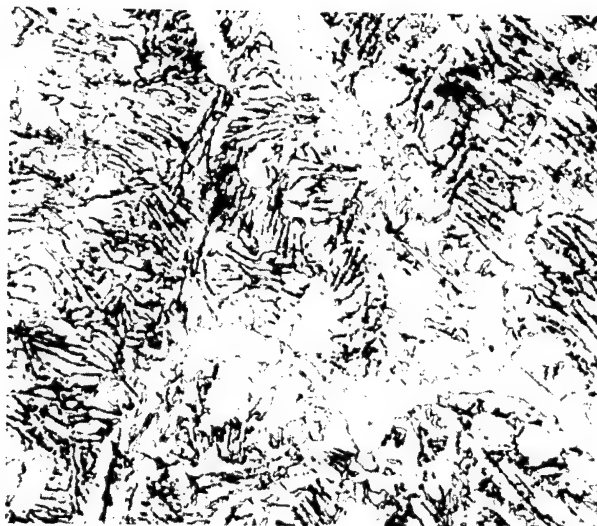


Fig. 33—Copper-zirconium alloy. 5.2% copper, 150X.



Fig. 34—Copper-zirconium alloy. 5.2% copper, 150X. Annealed and quenched at 850°C.

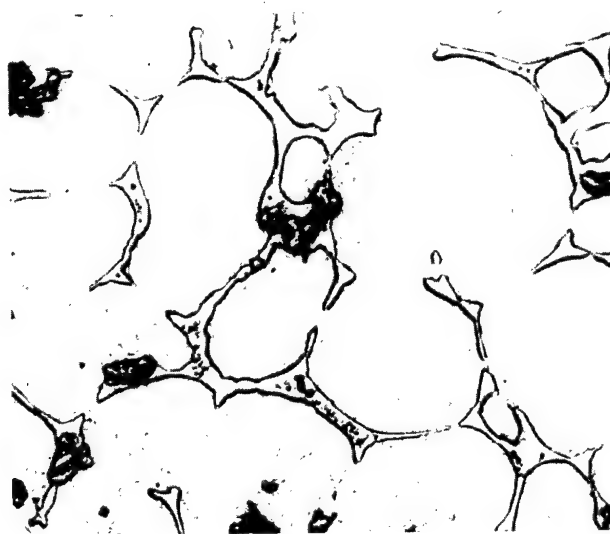


Fig. 35—Copper-zirconium alloy. 5.2% copper, 150X. Annealed and Annealed and quenched at 950°C.

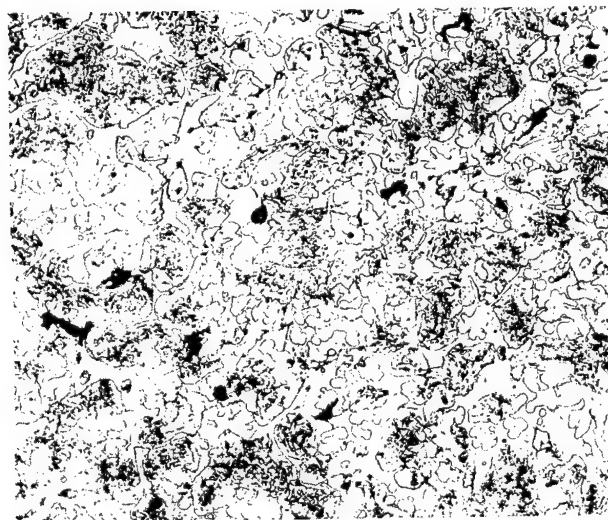


Fig. 36—Copper-zirconium alloy (bomb-reduced). 6.95% copper, 150X.

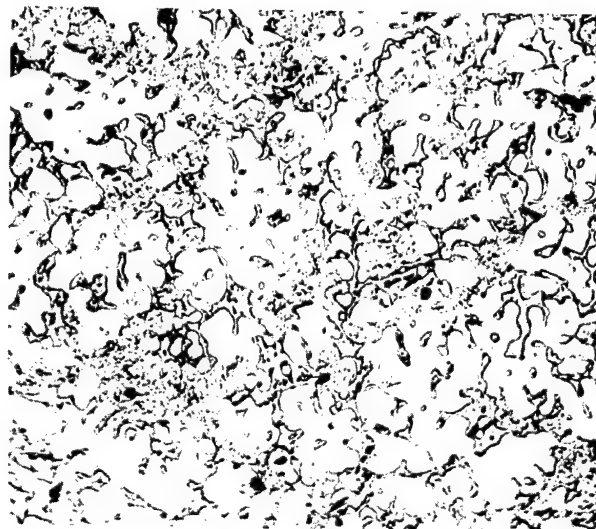


Fig. 37—Copper-zirconium alloy (bomb-reduced). 6.95% copper, 150X. Annealed and quenched at 850°C.

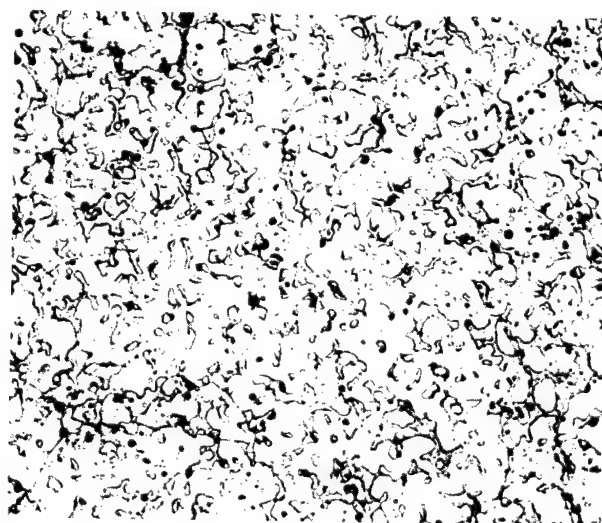


Fig. 38—Copper-zirconium alloy (bomb-reduced). 6.95% copper, 150X. Annealed and quenched at 900°C.

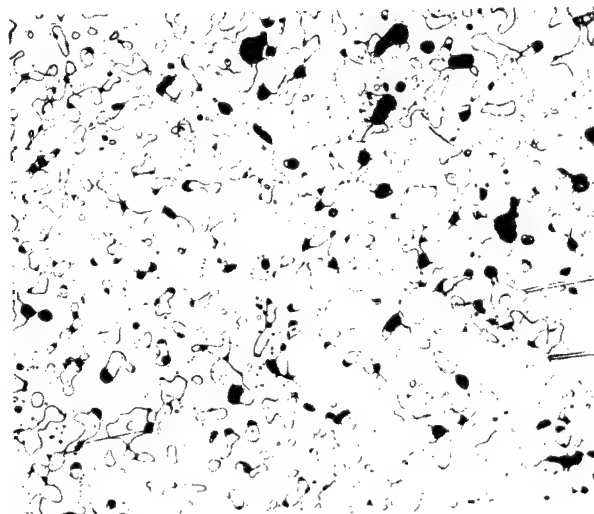


Fig. 39—Copper-zirconium alloy (bomb-reduced). 6.95% copper, 150X.
Annealed and quenched at 932°C.

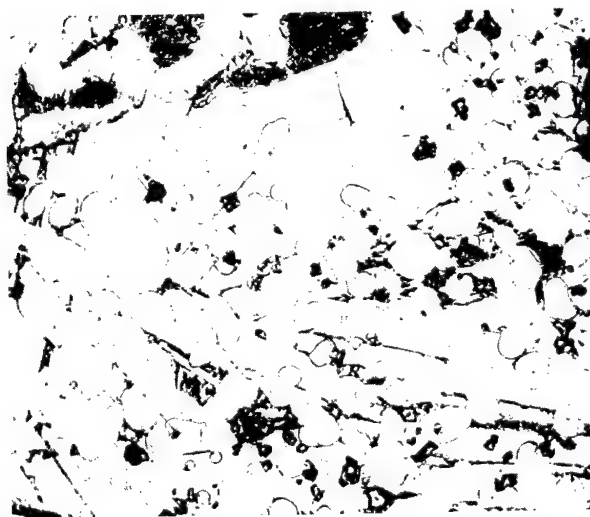


Fig. 40—Copper-zirconium alloy. 8.62% copper, 150X.

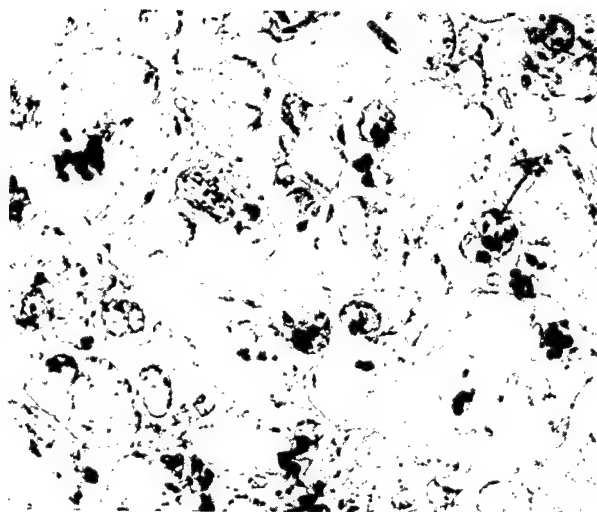


Fig. 41—Copper-zirconium alloy. 8.62% copper, 150X. Annealed and Annealed and quenched at 920°C.

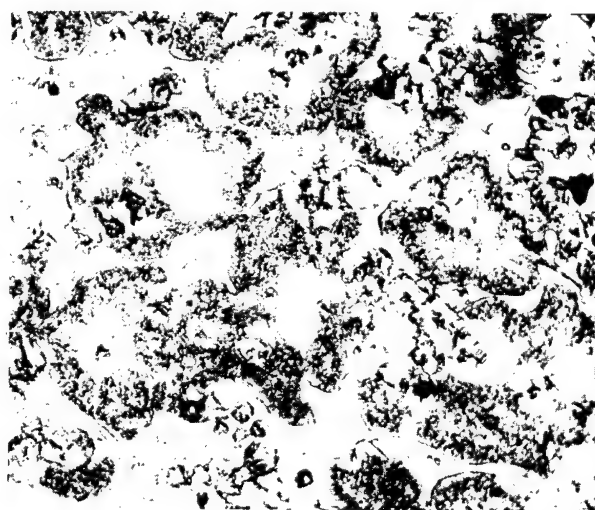


Fig. 42—Copper-zirconium alloy. 8.62% copper, 150X. Annealed and quenched at 950°C.

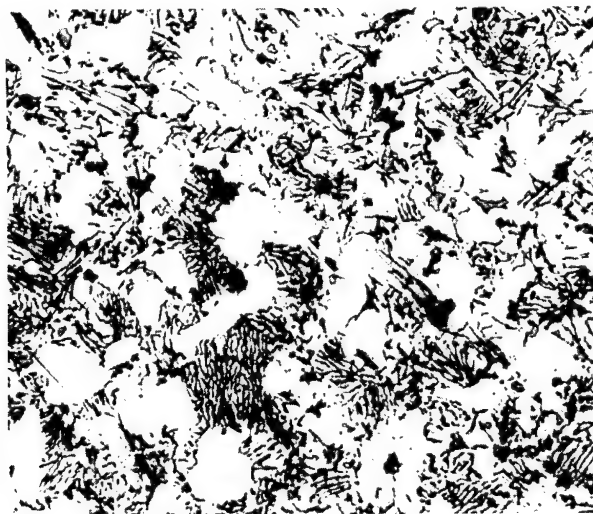


Fig. 43—Copper-zirconium alloy. 11.84% copper, 150X.

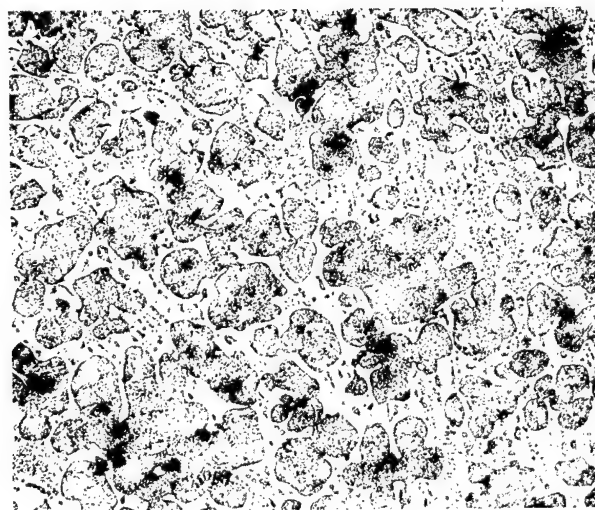


Fig. 44—Copper-zirconium alloy. 11.84% copper, 75X. Annealed and quenched at 950°C.

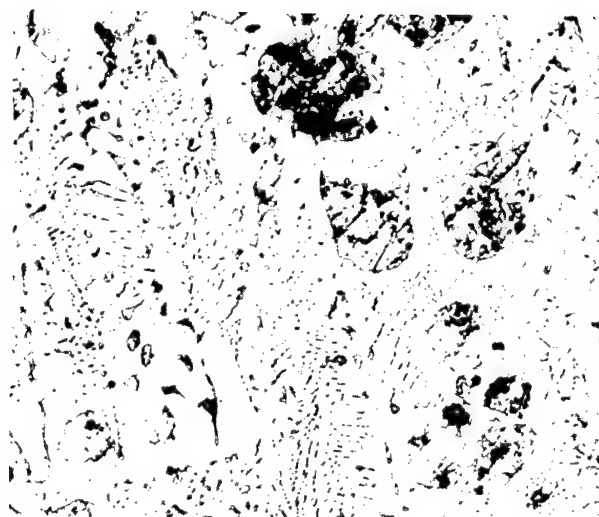


Fig. 45—Copper-zirconium alloy. 12.7% copper, 150X.



Fig. 46—Copper-zirconium alloy. 12.7% copper, 150X. Annealed and quenched at 854°C.

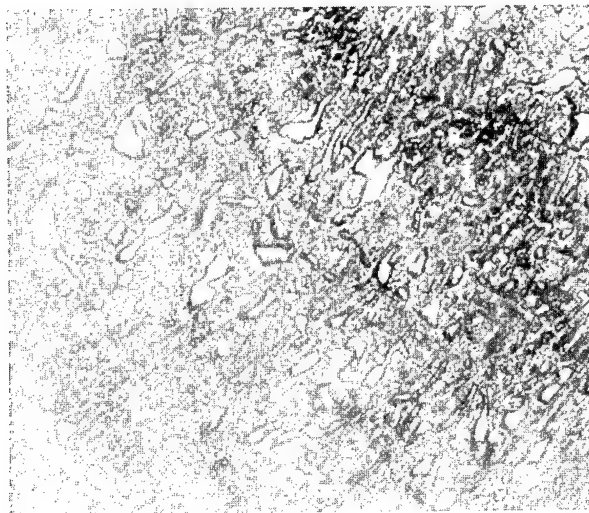


Fig. 47—Copper-zirconium alloy. 18.66% copper, 150X.

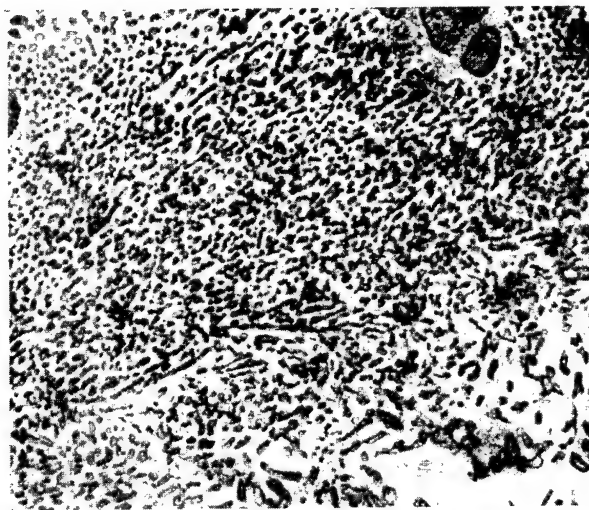


Fig. 48—Copper-zirconium alloy. 18.66% copper, 150X. Annealed and quenched at 854°C.

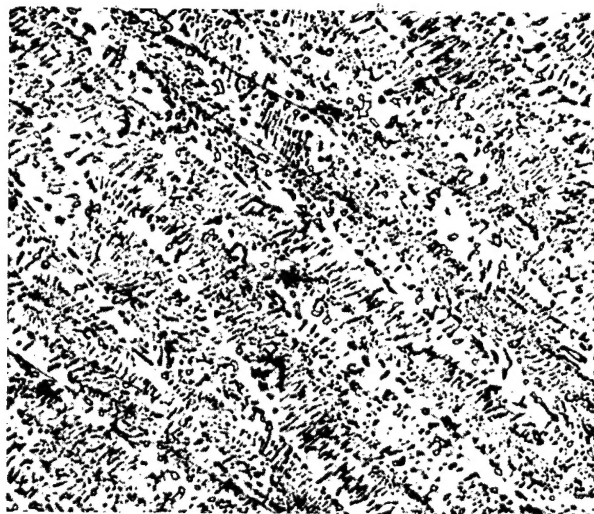


Fig. 49—Copper-zirconium alloy. 19.72% copper, 150X.

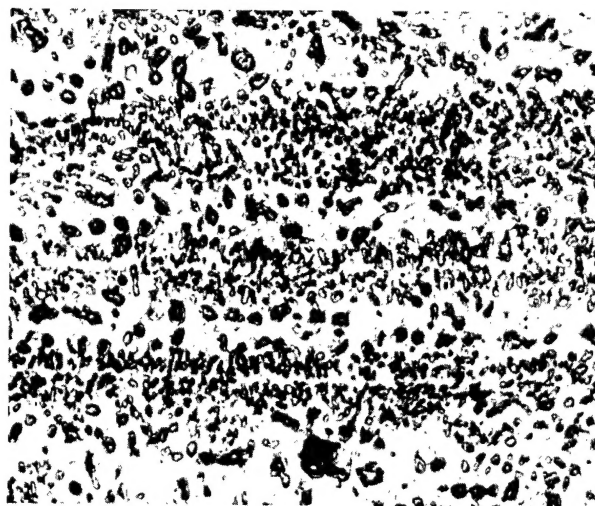


Fig. 50—Copper-zirconium alloy. 19.72% copper, 150X. Annealed and quenched at 854°C.

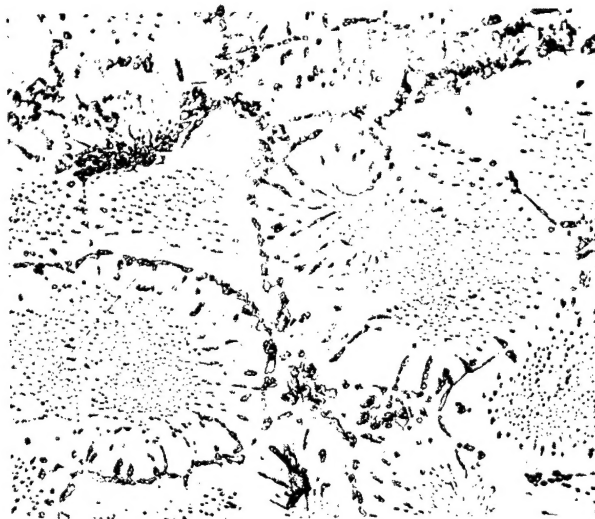


Fig. 51—Copper-zirconium alloy. 22.54% copper, 150X.

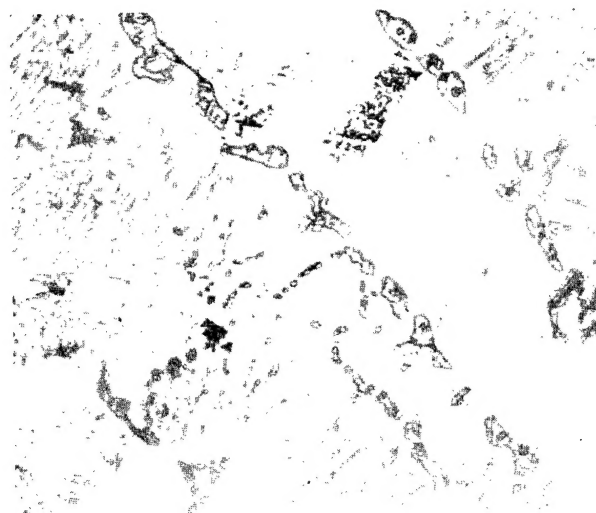


Fig. 52—Copper-zirconium alloy. 22.54% copper, 150X. Annealed and quenched at 854°C.

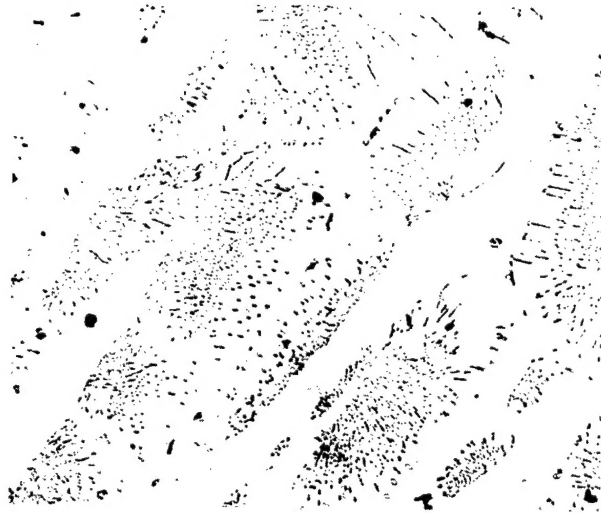


Fig. 53—Copper-zirconium alloy. 24.58% copper, 150X.



Fig. 54—Copper-zirconium alloy. 26.40% copper, 150X.

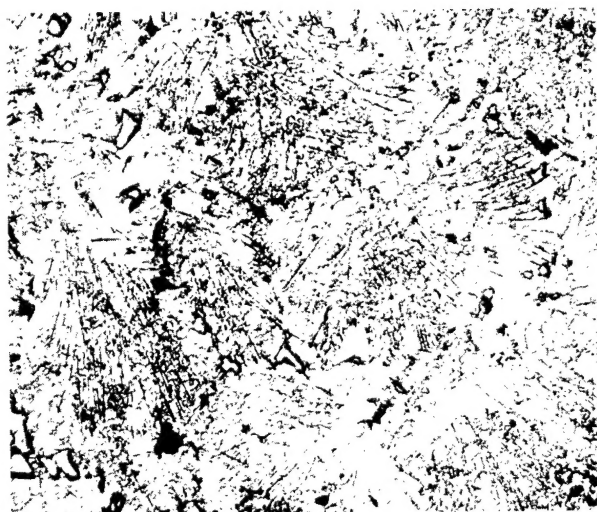


Fig. 55—Copper-zirconium alloy. 48.23% copper, 150X.